Geochimica et Cosmochimica Acta, Vol. 68, No. 24, pp. 5139–5150, 2004

0016-7037/04 $30.00 + .00

doi:10.1016/j.gca.2004.07.008

H_2O diffusion in dacitic and andesitic melts

HARALD BEHRENS,[1,*] YOUXUE ZHANG,[2] and ZHENGJIU XU[2]

[1]Institut für Mineralogie, UNI Hannover, Callinstr. 3, D-30167 Hannover, Germany
[2]Department of Geological Sciences, University of Michigan, Ann Arbor, MI 48109-1063, USA

(*Received January* 22, 2004; *accepted in revised form July* 1, 2004)

Abstract—The diffusion of water in dacitic and andesitic melts was investigated at temperatures of 1458 to 1858 K and pressures between 0.5 and 1.5 GPa using the diffusion couple technique. Pairs of nominally dry glasses and hydrous glasses containing between 1.5 and 6.3 wt.% dissolved H_2O were heated for 60 to 480 s in a piston cylinder apparatus. Concentration profiles of hydrous species (OH groups and H_2O molecules) and total water ($C_{H_2O_t}$ = sum of OH and H_2O) were measured along the cylindrical axis of the diffusion sample using IR microspectroscopy. Electron microprobe traverses show no significant change in relative proportions of anhydrous components along H_2O profiles, indicating that our data can be treated as effective binary interdiffusion between H_2O and the rest of the silicate melt. Bulk water diffusivity ($D_{H_2O_t}$) was derived from profiles of total water using a modified Boltzmann-Matano method as well as using fittings assuming a functional relationship between $D_{H_2O_t}$ and $C_{H_2O_t}$. In dacitic melts $D_{H_2O_t}$ is proportional to $C_{H_2O_t}$ up to 6 wt.%. In andesitic melts the dependence of $D_{H_2O_t}$ on $C_{H_2O_t}$ is less pronounced. A pressure effect on water diffusivity could not be resolved for either dacitic or andesitic melt in the range 0.5 to 1.5 GPa. Combining our results with previous studies on water diffusion in rhyolite and basalt show that for a given water content $D_{H_2O_t}$ increases monotonically with increasing melt depolymerization at temperatures >1500 K. Assuming an Arrhenian behavior in the whole compositional range, the following formulation was derived to estimate $D_{H_2O_t}$ (m^2/s) at 1 wt.% H_2O_t in melts with rhyolitic to andesitic composition as a function of T (K), P (MPa) and S (wt.% SiO_2):

$$\log D_{H_2O_t} = (-0.757 - 0.0868 \cdot S) + (-14,785 + 131.7 \cdot S)/T + (3.079 - 0.0490 \cdot S) \cdot P/T$$

The experimental data (69 in total, covering 803 to 1848 K and 0.1 to 1500 MPa) are reproduced by this relationship with a standard error of 0.12 log units. Using proportionality between water content and bulk water diffusivity, the above equation can also be used to estimate $D_{H_2O_t}$ in rhyolite to dacite containing up to 2 wt.% H_2O_t at magmatic temperatures. For andesitic melts the functional relationship between $D_{H_2O_t}$ and $C_{H_2O_t}$ is not known at magmatic temperatures and, hence, application of our model remains uncertain for such conditions. As the activation energy for water diffusion increases from rhyolite to andesite, the diffusivities become similar at intermediate temperatures. Below 1000 K (depending on H_2O content and pressure), water diffusion may be faster in rhyolite than in dacite than in andesite.

1. INTRODUCTION

Diffusion of H_2O in silicate melts and glasses plays a crucial role in degassing of magmas during volcanic eruptions. Whether magma degasses violently or effusively depends on various parameters, e.g., the melt viscosity, the concentrations of dissolved volatiles and their diffusivities. Understanding H_2O diffusion in magma is hence crucial to the understanding of volcanic processes such as bubble growth, magma degassing and magma fragmentation (Navon et al., 1998; Proussevitch and Sahagian, 1998; Zhang, 1999; Liu and Zhang, 2000; Martel et al., 2000, 2001). Compositions of magmas at subduction zones vary from rhyolitic to basaltic, although the liquid is often more silicic than the bulk magma. Hence, knowledge on H_2O diffusion behaviour is especially needed for silica rich melts to model volcanic eruptions. However, processes in the magma chamber before eruption might be also affected by H_2O diffusion, i.e., fluid-melt interaction and magma mingling and mixing. For instance, it has been suggested that the 1991 eruption of the Unzen volcano in Japan was initiated by a hot nearly aphyric andesitic magma penetrating into a colder partially crystallized dacitic magma (Holtz et al., in press). Several pieces of evidence indicate that the andesitic melt has a much lower water content (~4 wt.%) than the rhyolitic melt (~8 wt.%) in the overall dacitic magma. Diffusion of water in the melt is orders of magnitudes faster than Si and Al diffusion (Watson, 1994) and, hence, for a given time scale H_2O migrates much deeper into an adjacent melt than the other melt components (except of very fast elements such as sodium). The dissolved H_2O in turn reduces the melt viscosity and enhances the diffusion of the slow elements. Hence, it promotes mingling and mixing of both magmas. To understand and model bubble growth, degassing, and other volcanological and magmatic processes, H_2O diffusion data for melts of various compositions are required.

The diffusion of H_2O in natural rhyolitic melts has been studied extensively and is well understood (Shaw, 1974; Friedman and Long, 1976; Delaney and Karsten, 1981; Karsten et al., 1982; Lapham et al., 1984; Zhang et al., 1991; Nowak and Behrens, 1997; Zhang, 1999; Doremus, 2000; Zhang and Behrens, 2000). Shaw (1974) carried out the first study of H_2O diffusion in a rhyolitic melt. He demonstrated that H_2O diffusivity depends strongly on total dissolved H_2O content (hereafter referred to as H_2O_t), which was further verified in other studies (Friedman and Long, 1976; Jambon, 1979; Delaney and

* Author to whom correspondence should be addressed (h.behrens@mineralogie.uni-hannover.de).

Table 1. Composition of starting materials and a run product.

	DC dacite	PU andesite	AndDC2 dry half, centre	AndDC2 wet half, centre	AndDC2 wet half, rim
SiO_2	65.84	57.21	57.31	57.02	57.70
TiO_2	0.66	0.84	0.83	0.84	0.84
Al_2O_3	15.44	17.50	17.64	17.40	17.58
FeO^{total}	4.73	7.58	7.49	7.89	7.00
MnO	0.07	0.11	0.11	0.14	0.10
MgO	2.14	4.27	4.27	4.24	4.27
CaO	4.89	7.59	7.45	7.50	7.51
Na_2O	3.68	3.31	3.31	3.45	3.44
K_2O	2.55	1.60	1.58	1.53	1.56
H_2O_t	0.015[a]	0.018[a]	0.0[b]	3.2[b]	2.6[b]

Notes: Each listed composition is the average of at least 10 electron microprobe analyses. All iron is given as FeO. Analyses of DC and PU are from Ohlhorst et al. (2001). Data for H_2O_t based on IR spectroscopy are shown for comparison. Concentrations of all oxides except of H_2O are normalized to 100% total to facilitate comparison of wet and dry compositions.

[a] H_2O_t was determined by mid-infrared spectroscopy. Calibrations of Mandeville et al. (2002) for andesite and Yamashita et al. (1997) for dacite were used to convert the peak height of the 3550 cm^{-1} band into water content.

[b] H_2O_t was measured by near-infrared spectroscopy.

Karsten, 1981; Karsten et al., 1982; Lapham et al., 1984). Based on dehydration experiments with rhyolitic glasses containing up to 1.7 wt.% dissolved H_2O, Zhang et al. (1991) modelled the H_2O diffusion mechanism in rhyolitic melts by explicitly considering the role of water speciation in the melt. A result of their data processing was that the diffusion coefficient of OH groups is negligible and molecular H_2O is the diffusing species. They found that the diffusivity of molecular H_2O (hereafter referred to as H_2O_m) is roughly constant at low H_2O_t and the diffusivity of H_2O_t is proportional to H_2O_t content. Nowak and Behrens (1997) showed for haplogranitic melts compositionally similar to the natural rhyolites used by Zhang et al. (1991) that these diffusion laws cannot be extrapolated to high water content. At water contents < 3 wt.% a linear dependence of water diffusivity on H_2O_t was observed by Nowak and Behrens (1997), consistent with the findings of Zhang et al. (1991), but at higher water contents the water diffusivity varies exponentially with H_2O_t. Zhang and Behrens (2000) extended the study of H_2O in rhyolitic melts to high pressure (8.1 kbar) and high H_2O_t contents (7.7 wt.%). They developed a model to calculate water diffusivity in rhyolitic melts for a wide range of geological situations.

H_2O diffusion data in natural melt compositions others than rhyolite is scarce. Zhang and Stolper (1991) performed diffusion couple experiments with basaltic melts containing 0.04 to 0.4% H_2O_t at 1 GPa and 1573 to 1773 K. They found H_2O_t diffusivity in basaltic melt to be two orders of magnitude faster than in rhyolitic melt. Although H_2O_m concentration could not be directly measured, the observed proportionality between $D_{H_2O_t}$ and H_2O_t led them to suggest that molecular H_2O_m is also the diffusing species. Water diffusion in a trachytic melt was studied by Freda et al. (2003) in a piston cylinder at 1 GPa and 1373 to 1673 K. Using a Boltzmann-Matano analysis they found that $D_{H_2O_t}$ values increase linearly with H_2O_t up to 2 wt.%, and are intermediate between those in rhyolitic and basaltic melts at temperatures of ~1600 K. Recently, Liu et al. (2004) performed dehydration experiments with dacitic melts containing up to 2.5 wt.% H_2O_t at 824 to 910 K and ≤150 MPa. Their results contrast with the high temperature data for rhyolite and basalt in that H_2O_t diffusivity in the more depolymerized dacitic melt is slower than in the polymerized rhyolitic melt under the same conditions. Moreover, the dependence of $D_{H_2O_t}$ on $C_{H_2O_t}$ (total water content) is more pronounced in dacitic than in rhyolitic melts.

In this paper we examine the diffusion of H_2O in dacitic and andesitic melts at high temperature and pressure. Using our new experimental data, we evaluate the dependence of $D_{H_2O_t}$ on $C_{H_2O_t}$ for a couple of anhydrous melt compositions. Furthermore, by combining new and previous results, we attempt to discuss the mechanisms of H_2O diffusion, and to describe the compositional dependence of water diffusivity in these melts.

2. STARTING MATERIALS AND EXPERIMENTAL PROCEDURES

In the experiments, pairs of dry and hydrous glasses were combined to form a diffusion couple. Dry glasses with compositions close to the 1991 Unzen dacite and an earlier erupted Unzen andesite were synthesized by fusion of oxides and carbonates at 1873 K (Ohlhorst et al., 2001). Compositions are given in Table 1. Hydrous glasses were produced at high pressure by re-melting glass powder to which water was added. Syntheses of hydrous glasses were performed in platinum or gold-palladium capsules at 1523 to 1623 K and 500 MPa in an internally heated pressure vessel (IHPV). Sample assemblages were always H_2O-undersatured at run conditions so that water was completely dissolved in the melt. A rapid quench device was used to quench the melt to a crystal-free and bubble-free glass. Most of the hydrous glasses are from batches that were also used for the calibration of near-infrared absorption bands (Ohlhorst et al., 2001).

The air-molten andesite has an Fe^{3+}/Fe_{total} of 0.57, based on colorimetric measurement of FeO and microprobe analysis of total iron (Liebske et al., 2003). The hydrous glasses synthesized in the IHPV are more reduced. An Fe^{3+}/Fe_{total} of 0.33 was obtained for a synthetic andesitic glass containing 1.96 wt.% H_2O (Liebske et al., 2003). To examine the effect of the redox state of iron on the transport of H_2O, such as the role of molecular H_2, a reduced dry andesitic glass was prepared for two experiments (AndDC14 and AndDC15). Reduction was performed in a corundum crucible at ambient pressure in a tube furnace which was flushed with a gas composed by 93% Ar and 7% H_2 and saturated with H_2O at 20°C. Glass powder was slowly annealed at a rate of 1 K/min from 873 to 1523 K and then held as this temperature for 10 h to homogenize the melt. A small reaction rim between the melt and the crucible was formed, but the sample was cored from the center of the batch which was unchanged in composition. The quenched glass contains some bubbles. However, these bubbles are compressed in the high pressure experiments and are not visible in the diffusion samples. According to calculations after Kress and Carmichael (1991), if equi-

librium is reached, the Fe^{3+}/Fe_{total} ratio would be 0.026 at 1523 K. Redox state of iron in dacitic glasses was not analyzed.

Cylinders of 2.8 mm in diameter were drilled from the synthetic glasses and cut to a length of 2.5 mm. One of the base planes of each cylinder was polished. Two cylinders, one dry and one hydrous, were placed together so that the polished surfaces were in direct contact. In the first experiment (DacDC1), the couple was inserted in a platinum tube (3 mm inner diameter, 0.2 mm wall thickness) and the ends of the tube were closed and compressed using only pliers. However, it turned out that the melts are too fluid at the experimental temperature and the run product was deformed. In subsequent experiments the platinum capsule holding the diffusion couple was squeezed carefully to minimize trapped air and then welded shut. The sealed capsule was compressed in a cold-seal pressure vessel at room temperature with 50 MPa Ar pressure so that the platinum wall fits to the surfaces of the diffusion couple. The welded ends of the capsule were compressed carefully to reduce the length of the capsule to ~5.5 mm.

The experiments were performed in an end-load piston cylinder apparatus (PCA) at the University of Michigan. The sample assemblage (0.5 inches in diameter, 32 mm in length) consists of a $BaCO_3$ tube as the outer pressure medium, a graphite heater and crushable alumina as the inner pressure medium. The diffusion couple was placed in the center of the heater so that the interface was at the hottest point and the water-rich half was above the water-poor half. The temperature was measured on top of the sample using a type-D thermocouple (Re3W97-Re25W75).

A "piston-out" procedure was used to bring the assemblage cold to the final pressure. The assemblage was initially overpressurized by ~0.2 GPa and allowed to relax at 373 to 473 K for at least 5 h. Then the pressure was relaxed to the required pressure, and temperature was increased at a rate of 20 K/s or faster. Overshooting and fluctuation in temperature was <10 and <2 K, respectively. Runs lasted between 60 and 480 s. (A "zero-time" experiment was also run.) Cooling was initiated by turning off the heating power resulting in an initial quench rate of ~100 K/s. After the run, the diffusion-couple shows numerous cracks perpendicular to the cylindrical axis indicating non-hydrostatic stress during cooling. A slower rate in the final stage of cooling (100 K/s to 573 K and then 1 K/s to room temperature) did not prevent crack formation. Using a slower cooling rate from high temperature is ruled out to avoid formation of iron oxides, which can significantly change the background of the IR spectra (Liebske et al., 2003).

Calibrations of temperature gradient were performed at 0.5 GPa and 873 K using water speciation in a rhyolitic glass containing 0.9 wt.% H_2O_t (Ihinger et al., 1999) and at 1 GPa and 1673 K using the two-pyroxene thermometer after Nickel et al. (1985). Temperature gradients near the hot spots were found to be 10 K/mm at low temperature and 14 K/mm at high temperature (Tegge-Schüring, 2002). Since all our experiments were performed at high temperature, we have corrected the measured T using the value of 14 K/mm. The distance of the thermocouple to the interface of the diffusion couple was 2.5 ± 0.2 mm and, hence, 35 K were added to the measured T. The main change in $C_{H_2O_t}$ along the diffusion profiles occurs over a distance <1 mm and we estimate the uncertainty of temperature to be ~20 K including gradients, fluctuations and overshooting in temperature. The pressure uncertainty of the PCA is not exactly known, and it is roughly estimated to be 10% for pressures from 0.5 to 1.5 GPa.

As the run durations were very short, contributions to the diffusion profiles during heating and cooling have to be considered. We recorded the time-temperature history of each experiment by computer and calculated the effective run duration at the dwell temperature using preliminary estimates of the activation energy for bulk water diffusion (see Zhang and Behrens, 2000, for details of calculations). Typically, the correction amounts to 10 to 20 s added to the dwell to account for heating, cooling and overshooting, which is also confirmed by a "zero-time" experiment (AndDC10, Table 2). In this run the sample was immediately quenched after reaching the target temperature. Using effective run duration, the water diffusivity agrees within 30% with the prediction based on the high temperature experiments. In one experiment (DacDC6, Table 2), the power broke twice when reaching the target temperature. Hence, the time correction is much larger for this experiment.

3. ANALYTICAL PROCEDURES

Except for run DacDC1, samples show no significant deformation after the run. A slice was sectioned along the cylindrical axis of the diffusion couple and was polished on both sides to a thickness of 300 to 400 μm for IR measurements. The position of the interface often could be roughly estimated (±0.1 mm) in the sections by kinks at the edges caused by small offsets of the initial halves of the couple. Both halves are brown in color but the hydrous half is much more intensely colored. Inspections with an optical microscope show that the transition between both halves is planar and parallel to the original interface. This observation suggests that no significant convection takes place in the melt during experiment.

IR spectra were collected using an IR microscope Bruker IR scope II connected to an FTIR spectrometer Bruker IFS88 at University of Hannover. A slit aperture between the objective and the detector was used to limit the analyzed sample volume. In the focus plane, the area selected by the slit was 15 to 20 μm wide and 100 to 150 μm long. Spectra were recorded in the near-infrared using a tungsten light source, a CaF_2 beamsplitter and a narrow range MCT detector. Typically 50 to 100 scans were accumulated for each spectrum with a spectral resolution of 4 cm^{-1}. The near-infrared spectra of the dacitic and andesitic glasses after the run resemble spectra in Ohlhorst et al. (2001) and we have used their calibration to determine the concentrations of OH and H_2O_m from the peak height of the bands at 4500 and 5200 cm^{-1}, respectively. In doing so, linear baselines were fitted to both peaks (TT baseline according to Ohlhorst et al., 2001). This simple baseline correction is reliable to quantify H_2O_t (sum of H_2O molecules and water dissolved as OH) but may have systematic errors in the determination of hydrous species concentrations (cf. Ohlhorst et al., 2001).

To improve resolution of concentration measurement at low water contents, some profiles in andesitic samples were measured also by mid-infrared spectroscopy using a globar light source and a KBr beamsplitter. Other measurement conditions were the same as for near-infrared spectroscopy, except that a spectral resolution of 2 cm^{-1} was used. Here, $C_{H_2O_t}$ was calculated from the peak height of the 3550 cm^{-1} band using the calibration of Mandeville (2002).

The composition of selected samples was analyzed using an electron microprobe CAMECA SX 100. An accelerating voltage of 15 kV, a beam current of 4 nA and a defocused beam with 10 to 30 μm in diameter was used. Counting time was 2 s for Na and K and 5 s for the other elements.

4. EXPERIMENTAL RESULTS

All successful diffusion experiments are summarized in Table 2. Two other runs with andesitic composition at 1458 K/1 GPa and 1508 K/1 GPa failed because of partial crystallization. Extraction of iron from the melt into the platinum walls of the capsule was a minor problem in our experiments because run duration was short compared to cation diffusion rates in the melt (cf. Baker, 1990; Zhang, 1993; Kress and Ghiorso, 1995; Koepke and Behrens, 2001). Electron microprobe analyses in the center of sample AndDC2 show no significant difference in major element composition compared to the starting glass (Table 1). Slightly lower iron concentration was detected near

Table 2. Results of water diffusion experiments with dacitic and andesitic melts.

Sample	$C_{H_2O_t}$, max initial (wt.%)[a]	P (GPa)	$T_{meas.}$ (K)	T_{corr} (K)[b]	t_{dwell} (s)	$t_{eff.}$ (S)[c]	$C_{H_2O_t}$, max after run (wt.%)	$D_{H_2O_t}$ ($\mu m^2/s$) fit D = const.	$D_{H_2O_t}$ at I wt.% H_2O ($\mu m^2/s$) fit $D = C \cdot D^\circ$	$D_{H_2O_t}$ at 1 wt.% H_2O ($\mu m^2/s$) modified BM	Remarks
Dacite											
DacDC7	n.d.	1	1423	1458	300	311	4.7[d]	32.7 ± 4.1	**13.9 ± 1.9**	19 ± 6	Few crystals in dry half
DacDC5	n.d	1	1473	1508	300	309	4.6[d]	32.1 ± 3.9	**15.0 ± 2.1**	19 ± 4	
DacDC1	n.d	0.5	1573	1608	73	83	3.5[d]	53.7 ± 8.0	**36.6 ± 6.7**	47 ± 9	Sample slightly deformed
DacDC2	3.06	1	1573	1608	480	491	2.9[d]	43.0 ± 4.5	**35.5 ± 2.8**	38 ± 5	
DacDC3	5.60	0.5	1673	1708	120	133	6.2[d]	167 ± 17 (1^{st})	**65.7 ± 7.0**	85 ± 13	
								129 ± 13 (2^{nd})	**53.1 ± 6.2**	80 ± 12	
DacDC4	5.60	1.5	1673	1708	120	132	6.3[d]	209 ± 24	**78.4 ± 8.4**	98 ± 16	
DacDC6*	2.74	1	1763	1798	90	141	3.1[d]	161 ± 15	**110 ± 11**	128 ± 16	
Andesite											
AndDC10	n.d.	1	1523	1558	0	7.4	1.57[e]	(59 ± 30)	—	—	
AndDC2	n.d.	1	1573	1608	300	309	3.2[d]	121 ± 18	81.2 ± 9.0	**78 ± 11**	
AndDC15	n.d	1	1573	1608	300	320	1.57[e]	85 ± 7	—	**102 ± 11**	Reduced dry half used
AndDC3	6.3	1	1573	1608	120	131	5.6[d]	**112 ± 11**	63.6 ± 7.8	83 ± 21	
AndDC6	3.28	0.5	1673	1708	90	100	3.5[d]	171 ± 17	138 ± 16	**157 ± 16**	
AndDC5	3.28	1.5	1673	1708	90	101	3.5[d]	**202 ± 18**	104 ± 11	193 ± 18	
AndDC8	1.89	1	1773	1808	60	71	2.1[d]	215 ± 31	349 ± 47	**270 ± 39**	
AndDC14	n.d.	1	1773	1808	60	78	1.51[c]	**258 ± 24**	—	269 ± 25	Reduced dry half used
AndDC12	n.d.	1	1813	1848	126	140	1.59[e]	**487 ± 27**	—	525 ± 31	

Notes: Values in bold show the preferred diffusion data. Error of diffusivity is calculated by error propagation considering errors in run duration (5 s), in temperature (20 K), spatial resolution of the IR microscope (30 μm) and fitting error.

[a] Initial water content of the hydrous half is the average of Karl-Fischer titration measurements of the whole synthesized glass piece. KFT data are from Ohlhorst et al. (2001).

[b] T_{corr} refers to the temperature at the interface of the two halves of the diffusion couple. It is calculated from the measured temperature (T_{meas}) considering a gradient of 14 K/min.

[c] The effective run duration (t_{eff}) accounts for contributions to the diffusion profile during heating and cooling as well as for the small overshot in temperature in the beginning of the dwell.

[d] The mean water content near the concentration plateau in the water-rich half of the diffusion couple was determined by IR using the calibration for the TT baseline in Ohlhorst et al. (2001).

[e] Water content is based on the peak height of the 3550 cm^{-1} using the calibration of Mandeville et al. (2002).

* Heating power broke twice when approaching experimental temperature so that the time correction is about three times that for the other experiments.

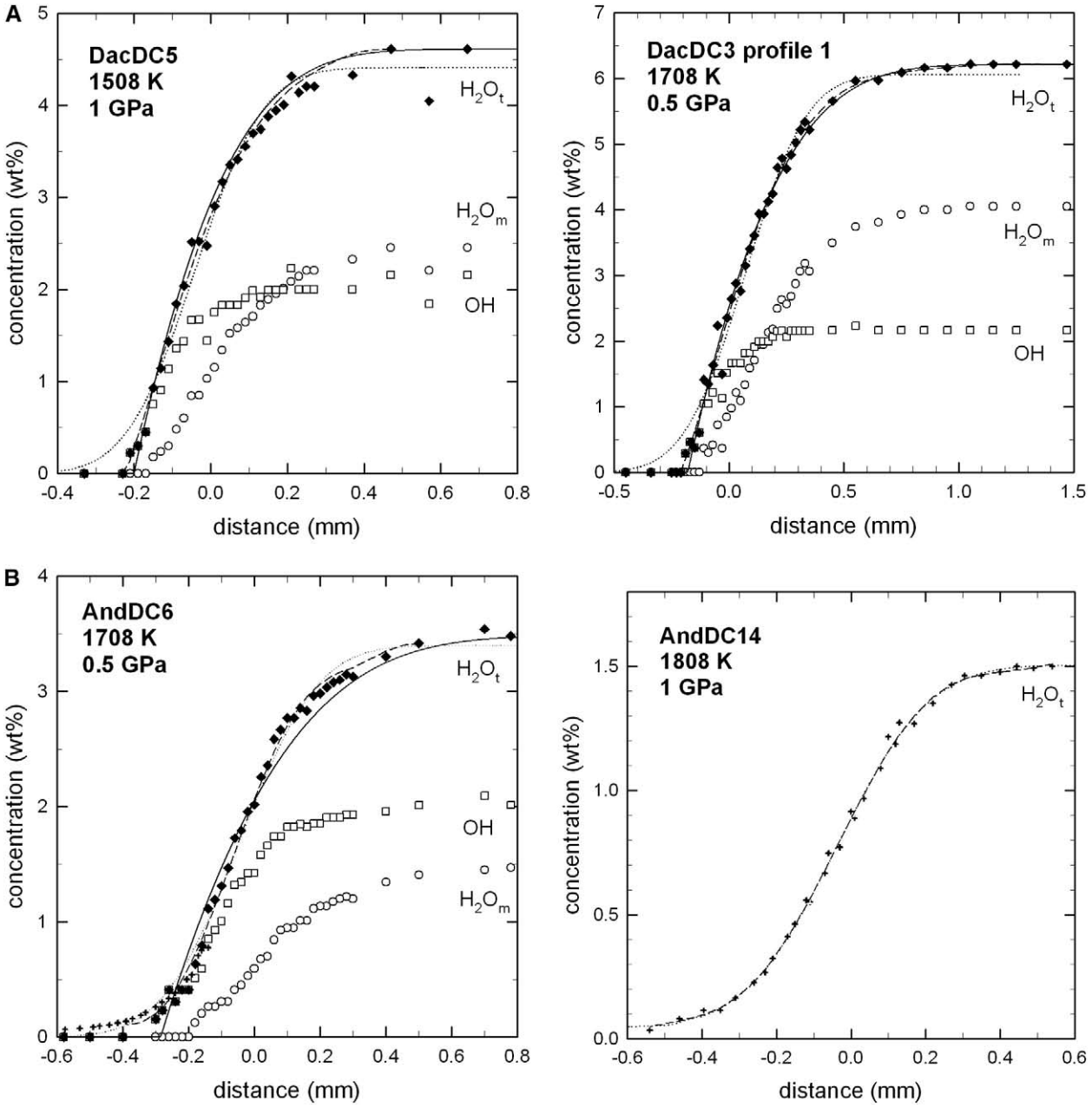

Fig. 1. Examples of total water concentration profiles in dacitic (A) and andesitic (B) melts. Only the central part of the profiles is shown for clarity. Solid curves are fits assuming bulk water diffusivity being proportional to $C_{H_2O_t}$. Dashed curves are seventh-order polynomial fittings used in the modified Boltzmann-Matano method. Dotted curves are error function fits assuming constant diffusivity. Black diamonds: H_2O_t from NIR spectroscopy, pluses: H_2O_t from MIR spectroscopy, open squares: OH, open circles: H_2O_m. Measurement of H_2O_t in andesitic glasses at low water content by MIR is more accurate than that at high water content by NIR, because of the complexity and low intensities of the NIR bands. The profiles of the two dacitic samples are well reproduced assuming water diffusivity being proportional to $C_{H_2O_t}$. In contrary, the H_2O_t profiles in andesitic samples is less dependent on water content and, hence, more symmetric.

the rim of the hydrous half, the effect of which on water diffusion is expected to be negligible.

Examples of diffusion profiles are shown in Figures 1. In the dry half the concentration of dissolved water was below the detection limit for the near-infrared combination bands (<0.1 wt.%). Scatter in concentrations of hydrous species as well as total water in the hydrous halves originates mostly from cracks in the diffusion couple. If the IR beam passes a crack in the sample, the measurements often yield too low concentrations. However, the number (<5 per mm) and width (<20 μm) of cracks was always low enough to enable a proper determination of the concentration-distance profiles. A decrease of H_2O_t near the end of the hydrous half was observed in some profiles (DacDC3-1, DacDC4, AndDC2, AndDC6) but in no

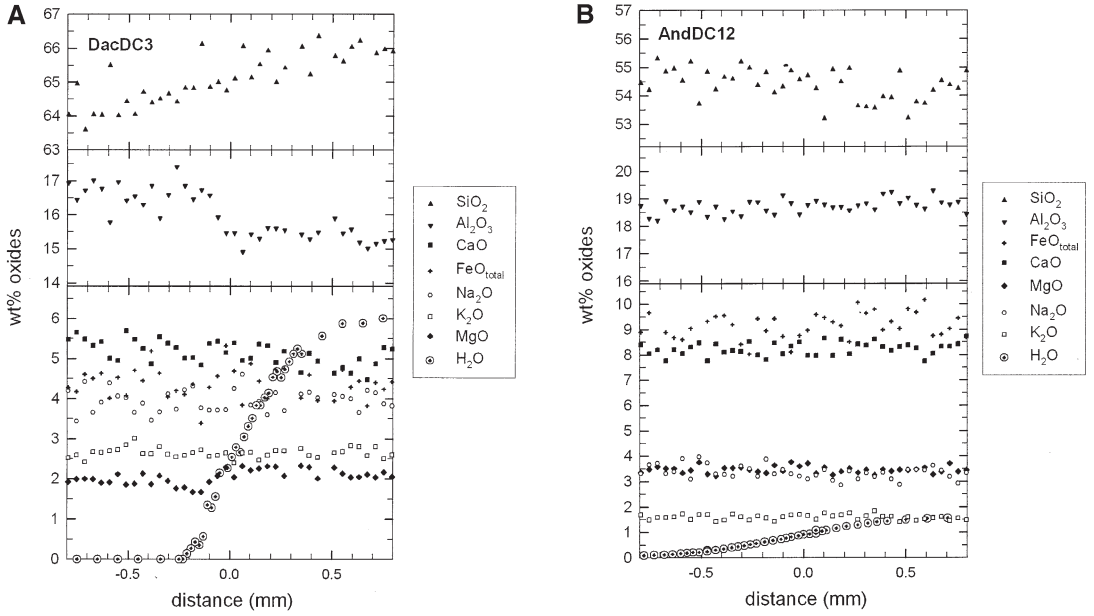

Fig. 2. Electron microprobe traverses along the H_2O_t profiles in a dacitic (A) and an andesitic (B) sample. Oxide contents are normalized to anhydrous composition to identify changes in relative abundance of cations. The H_2O_t profile measured by IR microspectroscopy is shown for comparison.

case the water-depleted zone extends to the diffusion profile between the dry and hydrous halves. An increase of H_2O_t at the end of the initially dry half was observed only in two experiment (DacDC2, AndDC14) indicating fast transport of H_2O along the capsule walls. However, this process affected only a small part of the sample near the rim and had no influence on the diffusion profiles measured in the center region of the couple.

The OH and H_2O_m concentrations measured in the glasses do not represent the equilibrium concentrations at the experimental conditions but are modified during cooling. Hence, we use the total water concentration profiles but not the relative abundance of hydrous species for modeling the diffusion process.

Two profiles were measured on sample DacDC3, profile 1 along the cylindrical axis and profile 2 parallel to the first profile near to the edge of the couple. Diffusion coefficients derived from both profiles are in good agreement giving further support that convection was not a problem in our experiments (Table 2).

5. DISCUSSION

5.1. Multicomponent Diffusion vs. Binary Interdiffusion

Dacite and andesite are multi-component systems and, hence, it is necessary to discuss whether multicomponent diffusion may have affected our experiments. It has to be emphasized that the purpose of this work is not to understand the multicomponent diffusion behavior in hydrous melts. Otherwise, it would be necessary to carry out many more experiments using diffusion couples with different anhydrous composition in the two halves, and compositional gradients in different couples would need to form roughly orthogonal vectors in the compositional space (Gupta and Cooper, 1971; Trial and Spera, 1994). To treat multicomponent diffusion fully requires the extraction of multicomponent diffusivity matrix. So far diffusion coefficient matrices were determined only for a few systems with 5 or more components: K_2O-Na_2O-Al_2O_3-SiO_2-H_2O (Mungall et al., 1998), and natural basaltic melt (Kress and Ghiorso, 1995). Due to the difficulty of extracting the diffusivity matrix for natural melts, simplified approaches have also been employed (e.g., Zhang, 1993).

The main purpose of our work is to understand H_2O diffusion in a fixed anhydrous composition, i.e., all components except H_2O are present in roughly the same relative proportion. One application of such data are to model bubble growth and degassing during volcanic eruption, when the concentration gradient is minimal if normalized to anhydrous basis. Because H_2O concentration gradient is the main gradient, its diffusion is expected to behave roughly as binary (Zhang et al., 1989). Invariant cation ratios observed along water diffusion profiles in rhyolitic melts (Zhang et al., 1991) and haplogranitic melts (Nowak and Behrens, 1997) support this suggestion.

To further verify the effect of other components on transport of H_2O, major oxide concentration profiles were determined. Figure 2 shows two examples of variations of major oxide components along the H_2O diffusion profiles. There is no significant variation in the relative abundance of cations for the andesitic sample AndDC14. That is, concentration gradient or diffusive flux of any anhydrous component due to H_2O diffusion is minimal and cannot be resolved within the precision of microprobe data. In the dacitic sample DacDC3, because of initial difference in the anhydrous composition of the two halves (due to imperfect preparation of the starting material), there are short diffusion profiles of Al_2O_3 and MgO (with 1 wt.% variation for Al_2O_3 and 0.5 wt.% for MgO), but no

variations in alkali concentrations. The molar change in MgO or Al_2O_3 concentration is more than one order of magnitude smaller than for H_2O. Hence, we conclude that for our H_2O diffusion experiments, coupling of H_2O to other components is of minor importance and H_2O transport can be treated as binary interdiffusion of H_2O and the rest of the silicate melt. However, it should be noted that the approach of effective binary interdiffusion only works when the anhydrous compositions in both halves of the diffusion couple are similar. For instance, H_2O_t profile between a dry rhyolitic melt and a hydrous basaltic melt may be strongly affected by the fluxes of the other components, and the diffusion problem may require dealing with multicomponent diffusion effects.

5.2. Possible Effect of Redox State of Iron on Water Transport

In previous studies on water diffusion in rhyolitic melt or synthetic FeO-free compositions, redox reactions did not play a role due to low FeO content. Because of the high total FeO concentration in our samples (especially the andesitic sample), the reaction

$$2FeO + H_2O = Fe_2O_3 + H_2 \quad (1)$$

might have influenced the H_2O profile. One possibility is hydrogen diffusion from the pressure medium into the diffusion capsule, which may interfere with the water diffusion profile. IR measurements show that the H_2O content in the dry half is unchanged relative to the initial glass for both dacitic and andesitic samples, except for a narrow rim (<200 μm in thickness) near the capsule wall. Hence, the region of the diffusion sample, where the profile is collected, is not affected by the pressure medium. The good agreement of diffusion coefficients extracted from profiles near the rim and in the centre line of sample DacDC3 gives further support of this conclusion.

A second, potentially more crucial, possibility is internal transport of molecular H_2 from the hydrous part to the anhydrous part. Such a profile would be superimposed on the measured H_2O profile and the effect would depend on the gradient in Fe^{3+}/Fe_{total}. In most of our experiments the dry glass was more oxidized (higher Fe^{3+}/Fe_{total}) than the hydrous glass. Because of the gradient in ferric and ferrous iron, molecular hydrogen may be released in the hydrous half, migrate into the dry half and react back to form H_2O and ferrous iron. This process would homogenize the ferric/ferrous ratio and transport H_2O from the hydrous to the anhydrous side. Estimation shows that H_2O_t would increase only by 0.2 wt.% in the dry half when the initial Fe^{3+}/Fe_{total} is reduced to the same value as in the hydrous half. This suggests that molecular hydrogen transport is of minor importance in most of our experiments. To further evaluate the role of hydrogen migration, two diffusion couple experiments were carried out in which a more reduced dry glass was used (AndDC14 and AndDC15). The diffusion data for these runs are in good agreement to the other data for andesitic melts (Table 2).

5.3. Modeling H_2O Diffusion

Different methods were applied to extract diffusion coefficients from the H_2O_t vs. distance profiles. First, the profiles were fitted assuming the diffusivity being constant. Next, the dependence of diffusivity on water content was analyzed using a modified Boltzmann-Matano method. Finally, the profiles were fitted assuming a functional relationship between diffusivity and water content.

5.3.1. Error Function Fit

Assuming a constant diffusivity D, the solution of Fick's second law for diffusion between two semi-infinite media with an initial concentration step at the interface is (Crank, 1975)

$$\frac{C - C_{min}}{C_{max} - C_{min}} = 1 - erf\left(\frac{x}{\sqrt{4Dt}}\right) \quad (2)$$

where C is the concentration at the distance x, C_{min} is the initial concentration in the dry half, C_{max} is the initial concentration in the hydrous half, and t is the time. Eqn. 2 fits the profiles in four andesitic couples (AndDC3, AndDC5, AndDC12 and AndDC14) quite well but all other profiles show systematic deviations to an error function fit (Fig. 1). It appears that deviation from error function shape in andesitic samples is especially pronounced at low water content and low temperature.

None of the dacitic samples is well reproduced by Eqn. 2 (Fig. 1). Profiles are steeper on the low H_2O_t side and extend deeper into the high H_2O_t side, indicating bulk water diffusivity increases with water content. This trend is consistent with findings on rhyolitic (Shaw, 1974; Zhang et al., 1991; Nowak and Behrens, 1997; Zhang and Behrens, 2000) and basaltic (Zhang and Stolper, 1991) melts.

5.3.2. Modified Boltzmann-Matano Analysis

To analyze the relationship between $D_{H_2O_t}$ and $C_{H_2O_t}$, the H_2O_t profiles were evaluated using the Boltzmann-Matano method modified by Sauer and Freise (1962):

$$D(x) = \frac{1}{-2t(\partial C/\partial x)_x}\left[(1 - C_x)\int_x^{+\infty} C dx + C_x\int_{-\infty}^{x}(1 - C)dx\right] \quad (3)$$

where C is the normalized concentration of H_2O_t (identical to the left hand side in Eqn. 2). As shown by Nowak and Behrens (1997) for haplogranitic melts, bulk water diffusivities determined by the approach of Sauer and Freise (1962) and by the original method of Boltzmann (1894) and Matano (1932–1933) are in very good agreement. A prerequisite for both methods is that change in density is minor along the profile. Density of glasses containing between 0 and 6 wt.% H_2O_t varies only by 4% for andesite and by 3% for dacite (Ohlhorst et al., 2001). In the melt the variation in density is probably slightly higher. Using the model of Ochs and Lange (1999) the density of andesitic melts containing 0 and 4 wt.% water differs by 8% at 1 GPa and 1573 K.

The approach of Sauer and Freise (1962) has two advantages compared to the original method of Boltzmann (1894) and Matano (1933): (1) the position of the Matano interface does not need to be found and (2) the precision is usually higher (Nowak and Behrens, 1997). To calculate the diffusion coefficients by the Sauer and Freise (1962) approach, profiles were fitted by seventh-order polynomials. The obtained diffusion

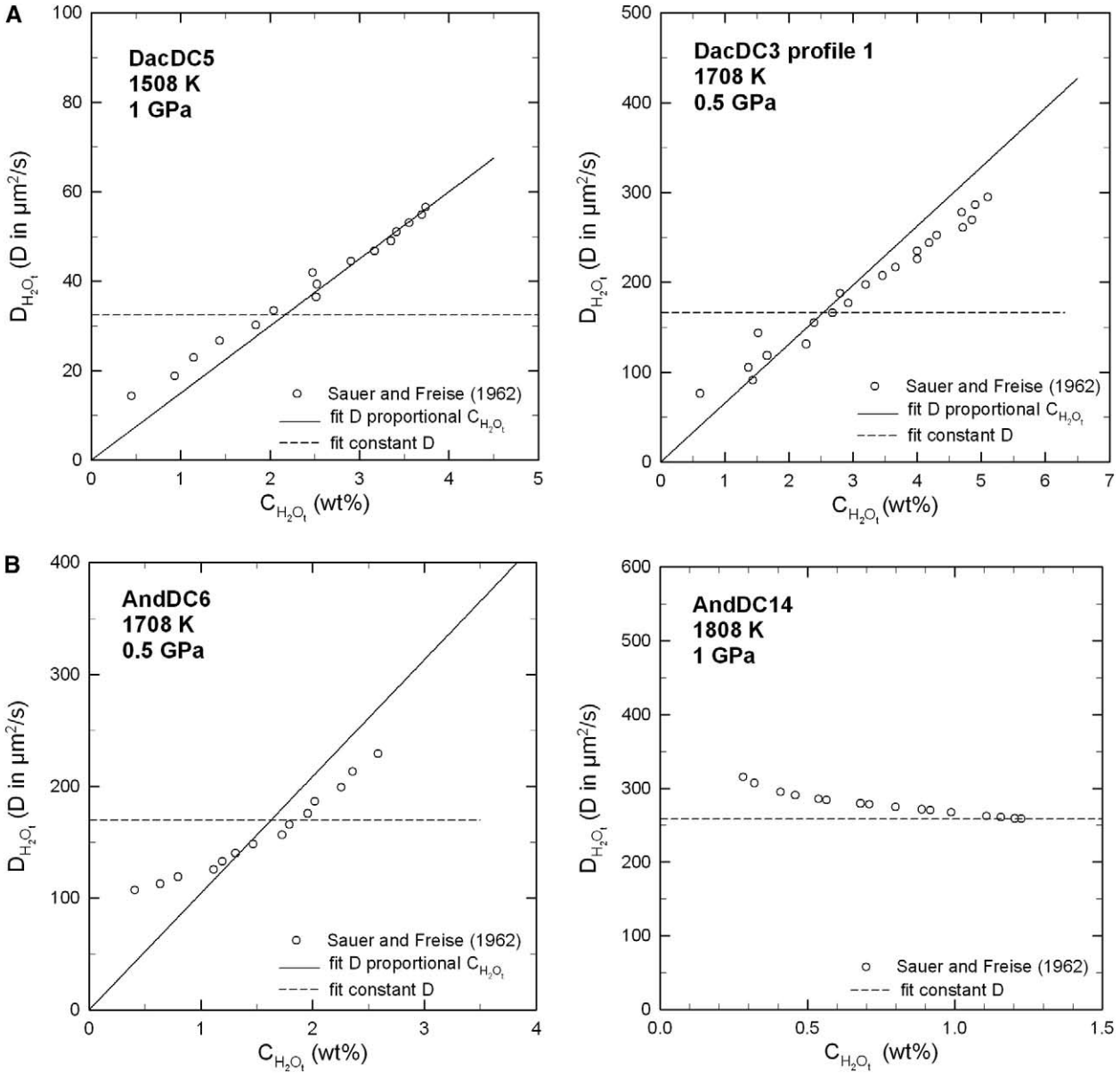

Fig. 3. Comparison of $D_{H_2O_t}$ vs. $C_{H_2O_t}$ derived using different evaluation methods for profiles shown in Figure 1.

coefficients as a function of water content are compared to data obtained by the other evaluation methods in Figure 3. Only between $C = 0.1$ and $C = 0.8$ the Sauer and Freise (1962) approach yield reliable diffusivities. Outside of this range, systematic errors due to polynomial fitting and to the scatter of the data produce very large errors in diffusivity and even the compositional trends for the diffusivity might be obscured. For dacitic melts, the results of the modified Boltzmann-Matano method are consistent with $D_{H_2O_t}$ being proportional to $C_{H_2O_t}$ in the whole range of water contents. For andesitic melts no significant dependence of $D_{H_2O_t}$ on $C_{H_2O_t}$ was found for runs AndDC3, AndDC5, AndDC12 and AndDC14 (Fig. 3), consistent with results from error function fitting. Other experiments indicate that the bulk water diffusivity in andesitic melts increases with total water concentration (AndDC6 is given as an example in Fig. 3).

5.3.3. Numerical Fitting of Diffusion Profiles

To verify the dependence of $D_{H_2O_t}$ on $C_{H_2O_t}$, the H_2O_t profiles were numerically fitted using functional relationships between diffusivity and total water concentration. The profiles in dacitic melts are well reproduced assuming

$$D_{H_2O_t} = C_{H_2O_t} \cdot D_{H_2O}^{1wt\%} \quad (4)$$

where $D_{H_2O_t}^{1wt.\%}$ is the bulk water diffusivity for 1 wt.% H_2O_t and $C_{H_2O_t}$ is in weight percent (Fig. 1A). The relationship originates from glass science literature (e.g., Doremus, 1973) and was

also applied to rhyolitic glasses using water speciation to model the bulk water diffusivity (Zhang et al., 1991). Eqn. 4 may not apply when $C_{H_2O_t}$ approaches 0 wt.% (such as parts per million level and below), because the relative abundance of the mobile species H_2O_m becomes negligible and diffusion of OH groups becomes the dominating mechanism for transport of water. Diffusion of OH groups bonded to tetrahedral cations (D_{OH}) is closely related to the dynamics of silicate network relaxation and is much slower than diffusion of H_2O molecules ($D_{H_2O_m}$), especially at low temperatures.

The dacitic profiles are well fit by assuming $D_{H_2O_t}$ being proportional to $C_{H_2O_t}$. On the other hand, the andesitic profiles show systematically deviations to the fit by assuming $D_{H_2O_t}$ being proportional to $C_{H_2O_t}$, i.e., at low water concentrations the calculated profile is steeper than the measured (Fig. 1c). Because of the obvious deviation between the fit and measured profile, only selected andesitic samples were fitted by Eqn. 4 (see Table 2).

5.4. *P-T-*$C_{H_2O_t}$ Dependence of Bulk Water Diffusivity

The simplest relationship to account for the effect of pressure and temperature on diffusion is the so called Arrhenius equation

$$D = D_0 \exp\left(-\frac{E_a + V_a P}{RT}\right) \quad (5)$$

where D_0 is a preexponential factor, E_a is the activation energy and V_a is the apparent activation volume. On a base-10 logarithmic scale this relationship translates to

$$\log D = a + \frac{b}{T} + \frac{cP}{T} \quad (6)$$

with parameters a, b and c being related to D_0, E_a, and V_a, respectively.

5.4.1. Dacite

The pressure effect on water diffusivity in dacitic melts is too small to be resolved properly by our experiments. At 1608 K identical $D_{H_2O_t}$ values of 36 $\mu m^2/s$ were obtained at 0.5 and 1.0 GPa. At 1708 K the diffusivity at 1.5 GPa (78 $\mu m^2/s$) is slightly higher than, and probably within error of, the average for the two profiles at 0.5 GPa (60 $\mu m^2/s$). Modeling of the diffusion profiles indicates that $D_{H_2O_t}$ is proportional to $C_{H_2O_t}$ at least up to 6 wt.% H_2O_t. In the H_2O_t range of 0 to 6 wt.% and in the temperature range of 1458 to 1798 K, $D_{H_2O_t}$ (m^2/s) can be calculated as a function of T (K) and $C_{H_2O_t}$ (wt.%) as

$$\log D_{H_2O_t} = \log C_{H_2O_t} - 5.93(\pm 0.33) - 7266(\pm 540)/T \quad (7)$$

1σ errors of fit parameters are given in parenthesis. This formula reproduces our experimental data for dacitic melts with a standard error of 0.06 log units. Extrapolated values of $D_{H_2O_t}$ at 600°C are 0.8 log units lower than data from Liu et al. (2004) based on dehydration experiments at pressures from 0.1 to 100 MPa (Fig. 4), suggesting a small negative effect of pressure on water diffusivity. However, because of the large extrapolation in temperature compared to the range in which the Arrhenius relationship was derived, this conclusion should be treated with caution.

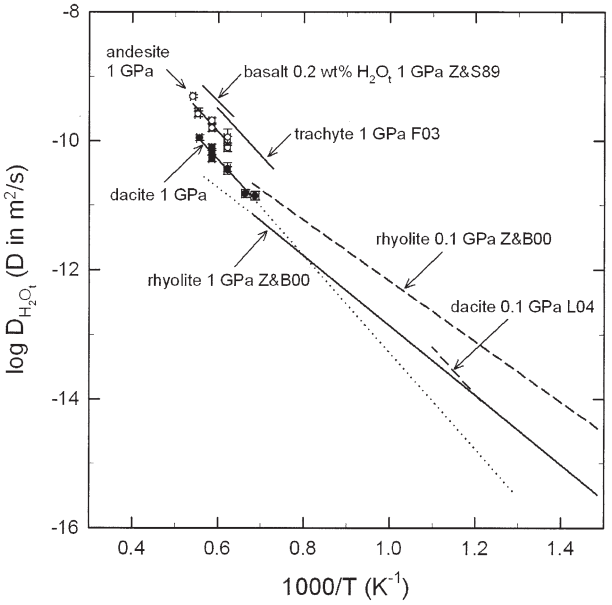

Fig. 4. Compilation of data for bulk water diffusivity in natural melts. Diffusion data are for 1 wt.% H_2O_t except for basalt (0.2 wt.% H_2O_t). Diffusivity in dacitic melts is based on fits of the profiles assuming $D_{H_2O_t}$ being proportional to $C_{H_2O_t}$. Diffusivity in andesitic melt was obtained by a modified Boltzman-Matano analysis or error function fitting (see Table 2). Solid lines correspond to 1 GPa and dashed lines to 0.1 GPa. Dotted lines are extrapolations in temperature. Data sources: basalt (Zhang and Stolper, 1991); rhyolite (Zhang and Behrens, 2000); dacite at low T (Liu et al., 2004); trachyte (Freda et al., 2003); other data (this work).

5.4.2. Andesite

Similar to the case of dacite, the pressure dependence of water diffusivity in andesite could not be clearly resolved from our data. The dependence of $D_{H_2O_t}$ with $C_{H_2O_t}$ in general is small and appears to vary with temperature and water content. Using the preferred data from Table 2 the following relationship was obtained for $D_{H_2O_t}$ at 1 wt.% H_2O_t in the range 1573 to 1813 K:

$$\log D_{H_2O_t} = \log C_{H_2O_t} - 5.41(\pm 0.54) - 7415(\pm 926)/T \quad (8)$$

The equation reproduces the experimental data with a standard error of 0.08 log units. However, extrapolation to magmatic temperatures (1100–1300 K) may lead to a large uncertainty. Moreover, the functional relationship between $D_{H_2O_t}$ with $C_{H_2O_t}$ can not be predicted for such conditions.

5.5. Comparison of Water Diffusivity in Natural Melts

Based on new results from this study and previous data, the dependence of $D_{H_2O_t}$ on $C_{H_2O_t}$ is summarized as follows:

1. For rhyolitic melt, over a wide range of conditions (673–1473 K, 0.1–810 MPa, and 0.1–7.7 wt.% H_2O_t), H_2O diffusion can be modeled by assuming H_2O_m is the only diffusing species and $D_{H_2O_m}$ depends exponentially on $C_{H_2O_t}$ (Zhang and Behrens, 2000). This exponential dependence of diffusivity of a molecular species has been verified by Ar diffusion in rhyolitic melts (Behrens and Zhang, 2001).

2. For dacitic melt, at low temperatures (773–913 K) and low pressures (<200 MPa), H_2O diffusivity depends more strongly on $C_{H_2O_t}$ than in rhyolite, and can be modeled by assuming H_2O_m is the only diffusing species and $D_{H_2O_m}$ depends exponentially on $C_{H_2O_t}$ (Liu et al., 2004). At high temperatures (1493–1798 K) and high pressures (0.5 to 1.5 GPa), H_2O diffusivity is roughly proportional to $C_{H_2O_t}$ (this work); that is, it depends less strongly on $C_{H_2O_t}$ than that in rhyolite. A proportionality between $D_{H_2O_t}$ and $C_{H_2O_t}$ can be interpreted as $D_{H_2O_m}$ being independent of $C_{H_2O_t}$ or weakly dependent on $C_{H_2O_t}$. In summary, both data sets for dacitic melts can be modeled by assuming H_2O_m is the only diffusing species and $D_{H_2O_m}$ depends exponentially on $C_{H_2O_t}$ at low temperature and weakly on $C_{H_2O_t}$ at high temperature.
3. For andesitic melt, there are no low-temperature diffusion data yet. At high temperatures (1608–1858 K), high pressures (0.5 to 1.5 GPa) and H_2O_t of 0.1 to 3.5 wt.%, $D_{H_2O_t}$ depends weakly on $C_{H_2O_t}$ (this work). Although the dependence of $D_{H_2O_t}$ on $C_{H_2O_t}$ is weak, it cannot be ruled out that at relatively low H_2O_t (e.g., 0.1–0.4 wt.%), $D_{H_2O_t}$ is roughly proportional to $C_{H_2O_t}$.
4. For basaltic melt, there are no low-temperature diffusion data yet. At high temperatures (1573–1773 K), 1.0 GPa, and H_2O_t of 0.04 to 0.4 wt.%, $D_{H_2O_t}$ is roughly proportional to $C_{H_2O_t}$ (Zhang and Stolper, 1991).

In summary, $D_{H_2O_t}$ increases from rhyolite to basalt at high temperatures, and decreases from rhyolite to dacite at low temperatures. $D_{H_2O_t}$ depends more strongly on $C_{H_2O_t}$ at low temperatures, and less on $C_{H_2O_t}$ at high temperatures. At low temperatures, $D_{H_2O_t}$ depends more strongly on $C_{H_2O_t}$ for less polymerized melt (dacite) than for more polymerized melt (rhyolite). At high temperatures, the trend is reversed, and the dependence of $D_{H_2O_t}$ on $C_{H_2O_t}$ decreases from polymerized melt (rhyolite) to depolymerized melt (basalt).

We do not yet have a perfect model to explain the complicated dependence of $D_{H_2O_t}$ on $C_{H_2O_t}$ and bulk composition of the melt summarized above. Additional experimental data to cover more *T-P-C* conditions are necessary, especially for depolymerized melts. Below we suggest some possibilities.

One explanation of the above results at high temperature is that molecular H_2O diffusivity increases with increasing $C_{H_2O_t}$ for rhyolitic and dacitic melts, and decreases slightly with increasing $C_{H_2O_t}$ for andesitic and basaltic melts. This explanation offers consistency in modeling H_2O diffusivity but it is against intuition that the addition of H_2O may decrease the diffusivity of hydrous species. One interesting test for this unusual model is to investigate how Ar diffusivity in andesitic and basaltic melts depends on $C_{H_2O_t}$.

Another possible explanation is that contributions of OH groups bonded to tetrahedral cations (D_{OH}) cannot be neglected in modeling the water diffusion profile for depolymerized melts at high temperatures. Estimated D_{OH} for andesitic melts using the Eyring relationship and viscosity data (Neuville et al., 1993; Richet et al., 1996) and assuming an effective jump distance of 3 Å, is 0.14 $\mu m^2/s$ at 1608 K and 2.2 $\mu m^2/s$ at 1808 K, respectively. These values are less than the measured bulk water diffusivities of this study by 2 to 2.8 orders of magnitude. Nevertheless, viscosity data have uncertainties and OH diffusivity estimated from viscosity may not be accurate. Direct determination of OH diffusivity (e.g., water diffusion at parts per million level of H_2O_t) are needed for hydrous iron-bearing andesitic melts to clarify a possible contribution of OH diffusion to $D_{H_2O_t}$.

A third possibility is contribution from "free" OH^- groups (OH^- groups not bonded to tetrahedral Si or Al) formed as follows:

$$H_2O + T\text{-}O^- = T - OH + OH^- \quad (9)$$

Recent ^1H MAS NMR measurements support the presence of such species in alkaline earth silicate glasses (Xue and Kanzaki, 2004). Reaction 9 offers the possibility of coupled diffusion of protons (via NBOs) and free hydroxide groups (via interstitial sites) (Scholze and Mulfinger, 1959; Haider and Roberts, 1970). A rapid motion of protons in depolymerized glasses can be inferred from impedance measurements on hydrous barium disilicate glasses (Behrens et al., 2002). No direct information is available about hydroxide diffusion in silicate melts, but Cl^- diffusion data (Watson, 1994) may shed some light on it.

5.6. Toward a Model to Predict H_2O Diffusivity in Rhyolitic to Basaltic Melts

In this section, we focus on the dependence of H_2O diffusivity on the anhydrous melt composition. There are not enough data for us to develop a comprehensive model on how H_2O diffusivity depends on the anhydrous melt composition. For andesite and basalt, the dependence of H_2O diffusivity on C_{H2Ot} is not known. Hence, we limit our discussion to rhyolitic, dacitic and andesitic melt at 1.0 wt.% H_2O_t, as a first step toward a model to predict the compositional dependence of H_2O diffusivity.

The compositional variation is expected to be complex due to the presence of many compositional components from rhyolite to dacite to andesite. Nevertheless, the available data only allow us to explore simple relations. Hence, as a first-order approximation, we use the SiO_2 content to represent the compositional variations. Figure 5 shows that log $D_{H_2O_t}$ at 1 wt.% H_2O_t varies almost linearly with the SiO_2 content from rhyolite to andesite. Extrapolated values for basalt are, however, much lower than the data experimentally found by Zhang and Stolper (1991) even for a lower water content. It is not clear how to extrapolate the diffusivity data at 0.04 to 0.4 wt.% H_2O_t to those at 1.0 wt.% (our new data on andesite do not support extrapolation based on proportionality) and, hence, we have not used these data in our calculation model.

Using the data summarized in Table 3 and assuming an Arrhenian behavior in the whole compositional range, the following formulation was derived to estimate $D_{H_2O_t}$ at 1 wt.% H_2O_t as a function of T (K), P (MPa) and S (wt.% SiO_2):

$$\log D_{H_2O_t} = (-0.757 - 0.0868 \cdot S) + (-14{,}785 + 131.7 \cdot S)/T + (3.079 - 0.0490 \cdot S) \cdot P/T \quad (10)$$

The experimental data (69 in total) are reproduced by this relationship with a standard error of 0.12 log units. Except of four experiments, deviation to the calculation is < 0.2 log units (Fig. 6). Eqn. 10 predicts that the pressure effect decreases from rhyolite to dacite and might be even positive for andesite.

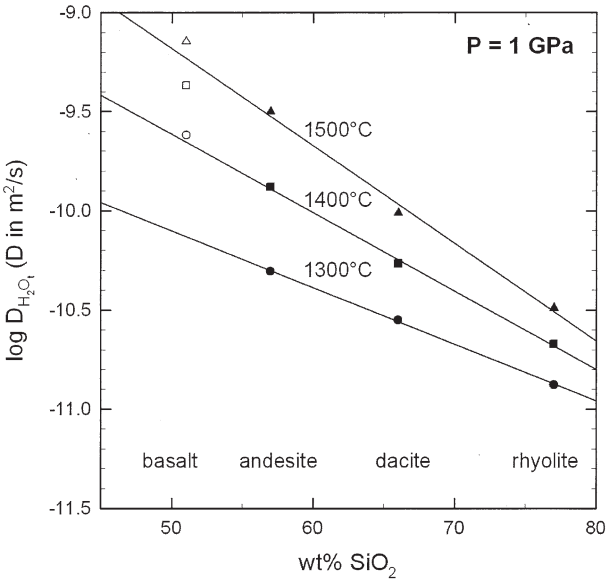

Fig. 5. Variation of bulk water diffusivity at 1 wt.% H_2O_t with SiO_2 content of the melt. Note that data for basalt at 0.2 wt.% H_2O_t (open symbols) from Zhang and Stolper (1991) are above the trend.

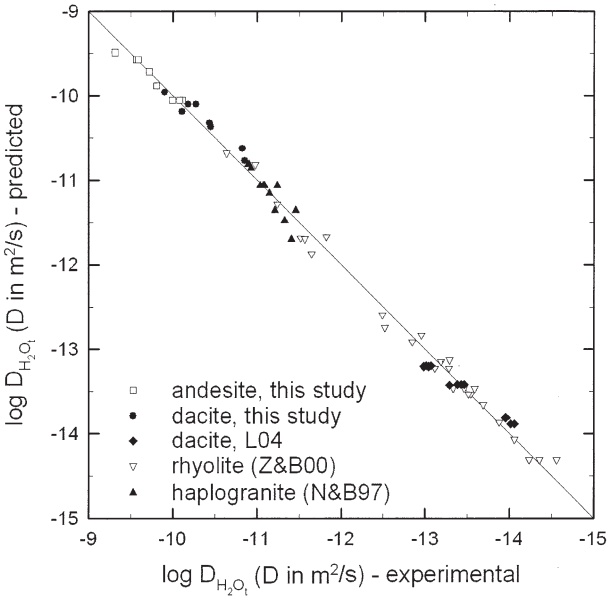

Fig. 6. Comparison of experimental bulk water diffusivities at 1 wt.% H_2O_t with predictions using Eqn. 10.

However, diffusion data at low temperature and pressure are required to verify the pressure dependence for andesite. Furthermore, because the temperature dependence of $D_{H_2O_t}$ increases from rhyolite to andesite, it is predicted that water diffusivity becomes similar in these melts at an intermediate temperature that depends on pressure (1450 K at 100 MPa and 950 K at 1 GPa). Below 1000 K (depending on H_2O content and pressure), water diffusion may be faster in rhyolite than in dacite than in andesite.

For rhyolite and dacite, Eqn. 10 is applicable in a wide pressure and temperature range as indicated in Table 3. It also allows interpolation of the diffusivity for intermediate compositions such as rhyodacite. Using the proportionality between water content and bulk water diffusivity, the above equation can also be used to estimate $D_{H_2O_t}$ in rhyolite to dacite containing up to 2 wt.% H_2O_t at magmatic temperatures. For andesitic melts the functional relationship between $D_{H_2O_t}$ and $C_{H_2O_t}$ is not known at magmatic temperatures and, hence, application of our model remains uncertain for such conditions. Moreover, diffusion data constraining the diffusivity of water for less silicic melts (<65 wt.% SiO_2) at temperatures < 1500 K is currently unavailable.

Applying the equation to other melt compositions is not recommended. Diffusion coefficients for trachytic melts in the same *P-T* range (Freda et al., 2003) are underestimated by 0.5 log units. This implies that water diffusion in alkali-rich melts is not well reproduced by our model.

6. IMPLICATIONS

This study provides important diffusivity data and equations for use by the volcanological community to model bubble growth and volcanic eruption dynamics of various magmas (Navon et al., 1998; Proussevitch and Sahagian, 1998), as well as magma chamber processes. The data can also be used to calculate rates for out-diffusion of water from hydrous rhyolitic to dacitic melts or for uptake of water from a fluid into a dry glass. For D proportional to C and constant initial concentration in the glass, the apparent diffusion-out diffusivity, $\bar{D}_{out}$, is given as $\bar{D}_{out} = 0.347 \cdot D_{H_2O_{t,max}}$, where $D_{H_2O_{t,max}}$ is the water diffusivity at maximum H_2O_t content of the melt (Zhang et al., 1991; Wang et al., 1996). The apparent diffusion-in diffusivity $\bar{D}_{in}$ is related to $D_{H_2O_{t,max}}$ as $\bar{D}_{in} = 0.619 \cdot D_{H_2O_{t,max}}$.

Future work includes the quantification of the pressure effect on H_2O diffusivity for dacite and andesite, especially at low temperatures (700–900 K). Furthermore, much more work is necessary to examine the effect of anhydrous melt composition so that a comprehensive model for H_2O diffusivity can be developed.

Table 3. Diffusivity data used to constrain Eqn. 10.

Composition	wt.% SiO_2	No. of data	P (MPa)	T (K)	$C_{H_2O_t}$ (wt.%)	Reference
Rhyolite	77	29	0.1–810	803–1488	0–7.7	Zhang and Behrens (2000)
Haplogranite	76	13	50–500	1173–1473	0–7.3	Nowak and Behrens (1997)
Dacite	67	12	0.1–140	824–911	0–2.5	Liu et al. (2004)
Dacite	67	8	500–1500	1423–1673	0–6.3	This study
Andesite	57	8	500–1500	1608–1848	0–5.6	This study

Acknowledgments—This research was supported by the German Science Foundation (DFG Be1720/7) and the US National Science Foundation (EAR-0125506, EAR-0228752). We thank O. Dietrich for preparation of sections for IR and N. Eilts for doing some IR measurements. Helpful comments from J. Mungall, M. Nowak and anonymous reviewer are acknowledged.

Associate editor: F. J. Ryerson

REFERENCES

Baker D. R. (1990) Chem. interdiffusion of dacite and rhyolite: Anhydrous measurements at 1 atm and 10 kbar, application of transition state theory and diffusion in zoned magma chambers. *Contrib. Mineral. Petrol.* **104,** 407–423.

Behrens H. and Nowak M. (1997) The mechanisms of water diffusion in polymerized melts. *Contrib. Mineral. Petrol.* **126,** 377–385.

Behrens H. and Zhang Y. (2001) Ar diffusion in hydrous silicic melts: Implications for volatile diffusion mechanisms and fractionation. *Earth Planet. Sci. Lett.* **192,** 363–376.

Behrens H., Kappes R., and Heitjans P (2002) Proton conduction in glass—An impedance and infrared spectroscopic study on hydrous $BaSi_2O_5$ glass. *J. Non-Cryst. Solids* **306,** 271–281.

Boltzmann L. (1894) Integration der Diffusionsgleichung bei variablen Diffusions-koeffizienten. *Ann. Phys.* **53,** 959–964.

Crank J. (1975) *The Mathematics of Diffusion*. Clarendon Press, Oxford, UK.

Delaney J. R. and Karsten J. L. (1981) Ion microprobe studies of water in silicate melts: Concentration-dependent diffusion in obsidian. *Earth Planet. Sci. Lett.* **52,** 191–202.

Doremus R. H. (1973) *Glass Science*. John Wiley, New York.

Doremus R. H. (2000) Diffusion of water in rhyolite glass: Diffusion-reaction model. *J. Non-Cryst. Solids* **261,** 101–107.

Freda C., Baker D. R., Romano C., and Scarlato P (2003) Water diffusion in natural potassic melts. *Geol. Soc. London Spec. Publ.* **213,** 53–62.

Friedman I. and Long W. (1976) Hydration rate of obsidian. *Science* **191,** 347–352.

Gupta P. K. and Cooper A. R. (1971) The [D] matrix for multicomponent diffusion. *Physica* **54,** 39–59.

Haider Z. and Roberts G. J. (1970) The diffusion of water into simple silicate and aluminosilicate glasses at temperatures near the transformation range. *Glass Technol.* **6,** 158–163.

Holtz F, Sato H, Lewis J, Behrens H., and, Nakada S (in press) Experimental petrology of the 1991-1995 Unzen dacite, Japan. Part I: Phase relations, phase chemistry and pre-eruptive conditions. *J. Petrol.*

Ihinger P. D., Zhang Y., and Stolper E. M. (1999) The speciation of dissolved water in rhyolitic melt. *Geochim. Cosmochim. Acta* **63,** 3567–3578.

Jambon A. (1979) Diffusion of water in a granitic melt: an experimental study. *Carnegie Institution Yearbook* 352–355.

Karsten J. L., Holloway J. R., and Delaney J. R. (1982) Ion microprobe studies of water in silicate melts: Temperature-dependent water diffusion in obsidian. *Earth Planet. Sci. Lett.* **59,** 420–248.

Koepke J. and Behrens H. (2001) Trace element diffusion in andesitic melts: An application of synchrotron X-ray fluorescence analysis. *Geochim. Cosmochim. Acta* **65,** 1481–1498.

Kress V. C. and Ghiorso M. S. (1995) Multicomponent diffusion in basaltic melts. *Geochim. Cosmochim. Acta* **59,** 313–324.

Lapham K. E., Holloway J. R., and Delaney J. R. (1984) Diffusion of H_2O and D_2O in obsidian at elevated temperatures and pressures. *J. Non-Cryst. Solids* **67,** 179–191.

Liebske C., Behrens H., Holtz F., and Lange R. A. (2003) The influence of pressure and composition on the viscosity of andesitic melts. *Geochim. Cosmochim. Acta* **67,** 473–485.

Liu Y. and Zhang Y. (2000) Bubble growth in rhyolitic melt. *Earth Planet. Sci. Lett.* **181,** 251–264.

Liu Y, Zhang Y., and, Behrens H (2004) H_2O diffusion in dacitic melt. *Chem. Geol.* **209,** 327–340.

Mandeville C. W., Webster J. D., Rutherford M. J., Taylor B. E., Timbal A., and Faure K. (2002) Determination of molar absorptivities for infrared absorption bands of H_2O in andesitic glasses. *Am. Mineral.* **87,** 813–821.

Martel C., Dingwell D. B., Spieler O., Pichavant M., and Wilke M. (2000) Fragmentation of foamed silicic melts: An experimental study. *Earth Planet. Sci. Lett.* **178,** 47–58.

Martel C., Dingwell D. B., Spieler O., Pichavant M., and Wilke M. (2001) Experimental fragmentation of crystal- and vesicle-bearing silicic melts. *Bull. Volcanol.* **63,** 398–405.

Matano C. (1932–1933) The relation between the diffusion coefficients and concentrations of solid metals (the nickel-copper system). *Jpn. J. Phys.* **8,** 109–113.

Mungall J. E., Romano C., and Dingwell D. B. (1998) Multicomponent diffusion in the molten system K_2O-Na_2O-Al_2O_3-SiO_2-H_2O. *Am. Mineral.* **83,** 685–699.

Navon O., Chekhmir A., and Lyakhovsky V. (1998) Bubble growth in highly viscous melts: Theory, experiments and autoexplosivity of dome lavas. *Earth Planet. Sci. Lett.* **160,** 763–776.

Neuville D. R., Courtial P., Dingwell D. B., and Richet P. (1993) Thermodynamic and rheological properties of rhyolite and andesite melts. *Contrib. Mineral. Petrol.* **113,** 572–581.

Nickel K. G., Brey G. P., and Kogarko L. (1985) Orthopyroxene-clinopyroxene equilibria in the system CaO-MgO-Al_2O_3-SiO_2 (CMAS): New experimental results and implications for the two pyroxene thermometry. *Contrib. Mineral. Petrol.* **91,** 44–53.

Nowak M. and Behrens H. (1997) An experimental investigation on diffusion of water in haplogranitic melts. *Contrib. Mineral. Petrol.* **126,** 365–376.

Ohlhorst S., Behrens H., and Holtz F. (2001) Compositional dependence of molar absorptivities of near-infrared OH- and H_2O bands in rhyolitic to basaltic glasses. *Chem. Geol.* **174,** 5–20.

Ochs F. A., III, and Lange R. A. (1999) The density of hydrous magmatic liquids. *Science* **283,** 1314–1317.

Proussevitch A. A. and Sahagian D. L. (1998) Dynamics and energetics of bubble growth in magmas: Analytical formulation and numerical modeling. *J. Geophys. Res.* **103,** 18223–18251.

Richet P., Lejeune A. M., Holtz F., and Roux J. (1996) Water and the viscosity of andesite melts. *Chem. Geol.* **128,** 185–197.

Sauer F. and Freise V. (1962) Diffusion in binären Gemischen mit Volumenänderung. *Z. Elektrochem. Angew. Phys. Chem.* **66,** 353–363.

Scholze H. and Mulfinger H. O. (1959) Der Einbau des Wassers in Gläsern. V. Die Diffusion des Wassers in Gläsern bei hohen Temperaturen. *Glastechn. Ber.* **32,** 381–385.

Shaw H. R. (1974) Diffusion of H_2O in granitic liquids, I, experimental data and II, mass transfer in magma chambers. In *Geochemical Transport and Kinetics* (eds. A. W. Hofmann et al.), pp. 139–170. Carnegie Inst. Wash., Washington, DC.

Tegge-Schüring A. (2002) *Cation Diffusion in Silicate Melts*. Ph.D. dissertation, Hannover, Germany.

Trial A. F. and Spera F. J. (1994) Measuring the multicomponent diffusion matrix: Experimental design and data analysis for silicate melts. *Geochim. Cosmochim. Acta* **58,** 3769–3783.

Wang L., Zhang Y., and Essene E. J. (1996) Diffusion of hydrous component in pyrope. *Am. Mineral.* **81,** 706–718.

Watson E. B. (1994) Diffusion in volatile-bearing magmas. *Rev. Mineral.* **30,** 371–411.

Xue X. and Kanzaki M. (2004) Dissolution mechanisms of water in depolymerised silicate melts: Constraints from ^{1}H and ^{29}Si NMR spectroscopy and ab initio calculations. *Geochim. Cosmochim. Acta* **68,** 000–000.

Yamashita S., Kitamura T., and Kusakabe M. (1997) Infrared spectroscopy of hydrous glasses of arc magma compositions. *Geochem. J.* **31,** 169–174.

Zhang Y. (1993) A modified effective binary diffusion model. *J. Geophys. Res.* **98,** 11901–11920.

Zhang Y. (1999) A criterion for the fragmentation of bubbly magma based on brittle failure theory. *Nature* **402,** 648–650.

Zhang Y. and Stolper E. M. (1991) Water diffusion in a basaltic melt. *Nature* **351,** 306–309.

Zhang Y. and Behrens H. (2000) H_2O diffusion in rhyolitic melts and glasses. *Chem. Geol.* **169,** 243–262.

Zhang Y., Walker D., and Lesher C. E. (1989) Diffusive crystal dissolution. *Contrib. Mineral. Petrol.* **102,** 492–513.

Zhang Y., Stolper E. M., and Wasserburg G. J. (1991) Diffusion of water in rhyolitic glasses. *Geochim. Cosmochim. Acta* **55,** 441–456.